

Magnetic studies of natural goethite samples from Tharsis, Huelva, Spain

Marcos A. E. Chaparro^{1,A}, Ana M. Sinito¹, Juan C. Bidegain² and Raúl E. de Barrio³

¹ CONICET and IFAS, Universidad Nacional del Centro de la Provincia de Buenos Aires (UNCPBA), Tandil, Argentina

² CIC - LEMIT, La Plata, Argentina

³ Instituto de Recursos Minerales, Universidad Nacional de La Plata (UNLP), La Plata, Argentina

Received: March 06, 2006; accepted: September 6, 2006

RESUMEN

Las propiedades magnéticas de la goethita no han sido ampliamente estudiadas. Las muestras naturales frecuentemente contienen mezclas complejas de minerales. En el presente trabajo se estudió material extraído de Tharsis (Huelva, España), con el propósito de corroborar la presencia de goethita, a partir de mediciones de magnetismo de rocas. A tal fin se realizaron mediciones de susceptibilidad magnética, magnetización remanente isotérmica (MRI), anhistérmica (MRA), y se efectuó la desmagnetización por campos alternos y por temperatura. Difracción de rayos X y microscopía de barrido electrónico también fueron efectuados.

Los resultados obtenidos son comparados y discutidos con relación a estudios previos de goethitas naturales y sintéticas. A partir de los estudios térmicos de MRI y no magnéticos, se observó la presencia de hematita magnéticamente más dura.

PALABRAS CLAVE: Goethita, hematita, magnetismo de rocas, magnetización remanente, Tharsis.

ABSTRACT

Magnetic properties of goethite have not been widely studied. Natural samples often contain complex mineral mixtures. Material from Tharsis (Huelva, Spain) is studied in order to corroborate the presence of goethite using rock magnetic measurements. Measurements of magnetic susceptibility, isothermal remanent magnetisation (IRM), anhysteretic remanent magnetisation (ARM), and magnetic and thermal demagnetisation were carried out. X-ray diffraction and scanning electron microscopy were also carried out.

The results are discussed and compared with previous studies of synthetic and natural goethites. The presence of magnetically harder hematite was observed from IRM, thermal and non-magnetic studies.

KEY WORDS: Goethite, hematite, remanent magnetisation, rock-magnetism, Tharsis.

INTRODUCTION

Goethite (α -FeOOH) is an orthorhombic antiferromagnetic iron hydroxide. It shows parasitic magnetisation due to defective spin compensation (Thompson and Oldfield, 1986; Banerjee, 1970; Hedley, 1971). This mineral is weakly magnetic. Goethite is a common component of some soils and sediments (within the so-called limonite group; Dunlop and Özdemir, 1997). This mineral is formed as a result of oxidative weathering and soil formation. Goethite, as other magnetic minerals, such as hematite and maghemite, occurs widely in many soils type (Mullins, 1977; Maher, 1986; Schwertmann, 1988; Liu *et al.*, 1993; Tarling and Hrouda, 1993; Hanesch *et al.*, 2006). It may be a product of water- or wind-transported erosion, *in situ* biogenic processes, and pedogenesis (Schwertmann, 1971; Taylor *et al.*, 1987; Fassbinder *et al.*, 1990; Evans and Heller, 1994; Fine *et al.*, 1995). Goethite commonly appears in soils as a breakdown product of magnetite, pyrite and iron carbonates or the hydration of hematite (Tarling and Hrouda, 1993).

This hydroxide has a very stable magnetisation at room temperature. Its Néel temperature (T_N) is 120°C, but studies carried out on different goethites show T_N variations from 60°C to 170°C depending on substitution (mainly Al-substitution), crystal defects, excess water, grain size, nonstoichiometry and modes of formation (Özdemir and Dunlop, 1996; De Boer and Dekkers, 1998; Dearing, 1999; Maher *et al.*, 2004; Barrero *et al.*, 2006). The specific magnetic susceptibility is between $26 \times 10^{-8} \text{ m}^3 \text{ kg}^{-1}$ and $280 \times 10^{-8} \text{ m}^3 \text{ kg}^{-1}$ (Thompson and Oldfield, 1986; Dekkers, 1989; Hunt *et al.*, 1995; Maher and Thompson, 1999; Walden *et al.*, 1999; Dearing, 1999).

Like hematite, goethite belongs to the group of “hard magnetic materials”, which need high magnetic fields in order to reach magnetic saturation. Although both minerals have similar remanent coercivities (see below), the saturation remanent magnetisation of goethite is obtained with higher magnetic fields. According to France and Oldfield. (2000), some samples containing goethite could not reach their saturation at fields of 10 T. Although Rochette and Fillion

(1989) found a negligible IRM up to 4 T in synthetic goethites, higher field measurements showed median acquisition field of 9-13 T and suggest saturation fields of 100 T. Recently, Rochette *et al.* (2005) found that some natural and synthetic goethite and hematite samples were unable to reach SIRM, even up to 20 T and 57 T. Rock magnetic techniques could underestimate the contribution of such minerals to remanent magnetisation.

Differentiation of goethite and hematite in mixed natural samples has been studied by different authors (e.g.: Stockhausen, 1998, France and Oldfield, 2000; Kruiver *et al.*, 2001; Sangode *et al.*, 2001; Sangode and Bloemendal, 2004; Maher *et al.*, 2004). Several rock magnetic experiments for identifying and discriminating both hard minerals have been proposed. Some of them are based on a combination of high-fields acquisition, analysis of IRM measurements, low and high temperature dependence of susceptibility, magnetic and thermal demagnetisation of remanence.

In this work natural goethite from Tharsis mine is magnetically investigated. Several rock magnetic studies at room temperature and high temperatures were performed in order to characterise this mineral and to consider the presence of other minerals, such as magnetite and hematite. Furthermore, X-ray diffraction (XRD) and scanning electron microscopy (SEM) supportive studies were carried out.

GEOLOGY

The Huelva Pyrite Province is located in the south-western region of Spain. Numerous Cu-Au bearing deposits are known as the Río Tinto mining district which has been exploited for about 3000 years. It constitutes a 50 km wide and 250 km long belt that extends from Sevilla, through Portugal, reaching almost the Atlantic coast. More than 75 mineralised sulphide-bearing bodies were identified. Río Tinto, Aznalcollar, Sotiel and Tharsis are among the best-known (Williams, 1933; Strauss and Madel, 1970; Williams *et al.*, 1975; Solomon *et al.*, 2002).

The Río Tinto mining district comprises a series of Upper Palaeozoic rocks (Devonian-Lower Carboniferous age), folded along an east-west axis bounded on the north by granodiorites of the Sierra Morena. The oldest unit in the Iberian pyrite belt is composed by slates and quartzites of Devonian age. Volcanic rocks that overlie the sedimentary sequence have been studied as two differentiated volcanic groups: a) a lower basic unit, integrated by basaltic, andesitic and pillow lavas of Tournaisian age and, b) an upper acid volcanic unit which includes rhyolites and dacites that are accompanied by a series of acid pyroclastic rocks of Tournaisian-Visean age (Figure 1). The latter are overlain by sediments, slates and quartzites, including turbidites of

Visean age (Culm). According to Dixon (1979) the whole sequence was folded in the late Carboniferous. The mineralization has been dominantly in the form of lenticular massive sulphide bodies, some of them associated with disseminated or stockwork zones.

The Tharsis mine (37° 42'N; 06° 35'E) presents volcanic-sedimentary concentrations of polymetallic sulphides, mostly pyrite with minor amounts of chalcopyrite, sphalerite, galena, gold and silver. The mineralised horizons are often evidenced by chert, jasperous materials and siliceous manganese levels.

The massive pyrite bodies were originally marked at outcrop by thick gossans (called "monteras" in Spain). These gossans are an open-textured mixture of irregular and concretionary masses of siliceous hematite cemented by limonite material. The "monteras" seem to contain lepidocrocite together with goethite producing pseudomorphic replacements on pyrite crystals by supergene alteration.

SAMPLE AND MEASUREMENT TECHNIQUES

A natural sample named Goeth1 from Tharsis mine (Figure 1) was prepared in our laboratory, packed and fixed in plastic and Pyrex glass containers (~8 cm³), and then subjected to magnetic studies: magnetic susceptibility (κ), ARM, IRM, alternating field demagnetisation (AF), and thermal studies. In order to carry out IRM, ARM and thermal measurements, the samples were consolidated with a sodium silicate solution.

Magnetic susceptibility was measured with a magnetic susceptibility meter MS2, Bartington Instruments Ltd., linked to MS2B dual frequency sensor (0.47 and 4.7 KHz), with a precision of about 1%. With this sensor, it is possible to measure specific susceptibility χ ($\chi = \frac{\kappa}{\rho}$), and also low field κ in two frequencies ($\kappa_{4.7}$ and $\kappa_{0.47}$), so it was possible to estimate frequency-dependent parameter (Dearing *et al.*,

1996; Mullins, 1973) $\left(\kappa_{FD} \% = \frac{\kappa_{0.47} - \kappa_{4.7}}{\kappa_{0.47}} \times 100 \right)$. Another

interesting study to take into account is temperature dependence of κ . This study was carried out with an adapted device for the susceptibilimeter, developed in our laboratory, i.e. a furnace to heat the samples (from room temperature to 700°C), a thermometer and a thermal isolator to protect the MS2B sensor. The process was carried out in air. The heating rate was 10°C min⁻¹.

Measurements of ARM and partial ARM (pARM) were carried out with an optional pARM device attached to an alternating field demagnetizer Molspin Ltd. and a spinner

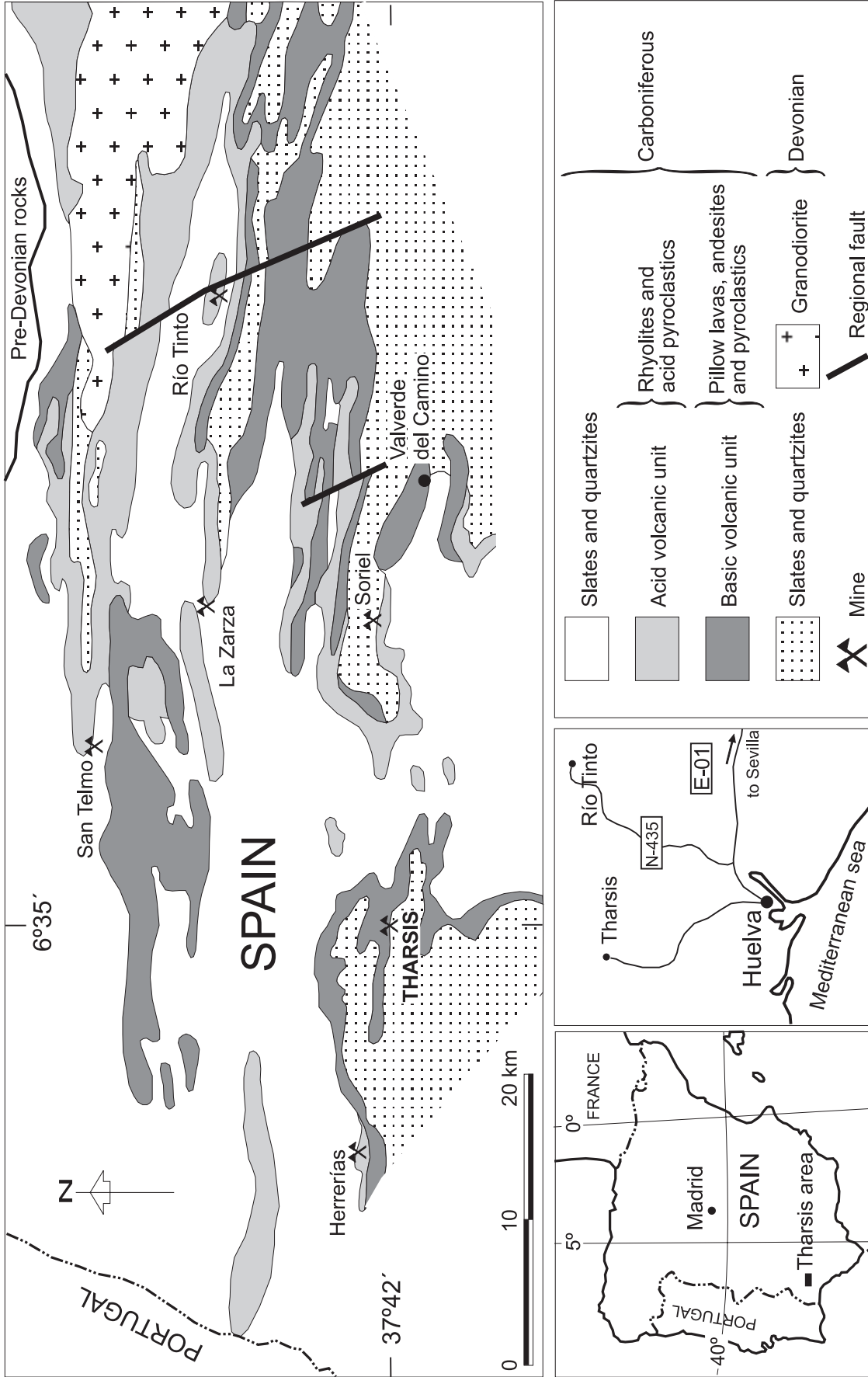


Fig. 1. Location map from Tharsis, Huelva Province, Andalucía, Spain.

fluxgate magnetometer Minispin, Molspin Ltd. with a precision of about 5%. For both measurements the peak AF was 100 mT. ARM was determined superimposing a DC bias field of 90 μ T. In order to calculate the anhysteretic susceptibility κ_{ARM} , DC field ranged between 10 and 90 μ T. The studies of pARM were done with a rate of decrease of 17 μ T per cycle and applying a DC field of 50 μ T over specific AF windows. A width of 5 mT for the window (it was moved into a range between 2.5 and 100 mT) was chosen, in order to find the coercivity spectrum.

IRM studies were conducted by using a pulse magnetizer model IM-10-30 ASC Scientific and the above mentioned magnetometer. Each sample was magnetized by exposing to growing stepwise DC fields with the magnetizer (from 10 mT to 4.5 T) and the remanent magnetisation, after each step, was measured using the magnetometer. After reaching IRM at a high field of 4.5 Tesla ($\text{IRM}_{4.5\text{T}}$), backfield was applied, in order to find the necessary field to eliminate the $\text{IRM}_{4.5\text{T}}$, coercivity of remanence (H_{CR}). Another parameter, related to contribution of hard magnetic minerals (antiferromagnetic, e.g.: goethite, hematite) and soft magnetic minerals (ferrimagnetic, e.g.: magnetite), is S-ratio, defined as $\text{IRM}_{300\text{mT}}/\text{IRM}_{2.4\text{T}}$, where $\text{IRM}_{300\text{mT}}$ is the acquired IRM at a backfield of 300 mT.

After reaching ARM and $\text{IRM}_{2.4\text{T}}$ the samples were demagnetised using an AF demagnetiser Molspin Ltd. with the highest peak value of 102.5 mT. The median destructive fields (MDF) were also calculated for both remanences.

Thermal demagnetisation was carried out with the thermal specimen demagnetiser, model TD-48 ASC Scientific. Samples were heated in growing stepwise temperatures in air, from room temperature up to 700°C. After each step, remanent magnetisation and magnetic susceptibility were measured for cooled samples. Thermal demagnetisation and susceptibility curves were represented.

The identification of minerals by X-ray diffraction was performed with a Philips PW 1027 diffractometer using $\text{Cu-K}\alpha$ radiation, Ni filter and velocity of scanning $^{\circ}2\theta/\text{minute}$.

RESULTS AND DISCUSSION

Magnetic susceptibility was measured twice and then averaged (Table 1), the value of χ was $38.9 \times 10^{-8} \text{ m}^3 \text{ kg}^{-1}$. Such value of magnetic susceptibility is within the range proposed by different authors (Thompson and Oldfield, 1986; Dekkers, 1989; Hunt *et al.*, 1995; Maher and Thompson, 1999), as can be observed in Table 1. On the other hand, frequency-dependent magnetic susceptibility ($\kappa_{\text{FD}}\%$) was 0%. This value rules out the presence of materials with superparamagnetic domains (SP).

The measurements of pARM showed low acquisition values (between 4.7 and 5.4 mA m^{-1}), and non-significant relative variations of pARM ($\sim 15\%$). Therefore no definitive conclusions have been achieved. Generally these variations are related to magnetites of different grain size (Jackson *et al.*, 1988). Probably, the lack of conclusions in this case is due to the antiferromagnetic characteristics of the sample, in view of the fact that the spectrum of coercivities is different from those of soft magnetic materials (ferrimagnetic).

Figure 2 shows the acquired ARM at several applied DC fields; the highest value of ARM was $\sim 33.9 \text{ mA m}^{-1}$ ($19.4 \times 10^{-6} \text{ A m}^2 \text{ kg}^{-1}$). The response of the materials is almost lineal; the correlation factor of a lineal fitting is excellent ($R \sim 0.99$). The slope of the straight line defines the κ_{ARM} and it is $27.1 \times 10^{-5} \text{ SI}$ ($15.5 \times 10^{-8} \text{ m}^3 \text{ kg}^{-1}$). The value of ARM ($\text{ARM}_{90\mu\text{T}}$) is of the same order of magnitude as those reported by other authors (Table 1). In addition, two ratios between different parameters ($\text{ARM}/\text{IRM}_{2.4\text{T}}$, ARM/χ) are also within the range of characteristic values of natural goethite (Table 1).

IRM acquisition and backfield measurements are shown in Figure 3. The natural remanent magnetisation (NRM) of the sample was $\sim 3.5 \times 10^{-6} \text{ A m}^2 \text{ kg}^{-1}$. High fields ($\sim 4.5 \text{ T}$) were not enough to reach the saturation IRM (SIRM), $\text{IRM}_{4.5\text{T}} = 39.2 \text{ A m}^{-1}$. ($22.2 \text{ mA m}^2 \text{ kg}^{-1}$). Values of SIRM for natural goethite reported by other authors ($\sim 8 \text{ mA m}^2 \text{ kg}^{-1}$, France and Oldfield, 2000, $\sim 50 \text{ mA m}^2 \text{ kg}^{-1}$, Maher and Thompson, 1999) are of the same order of magnitude as those recorded in this work for $\text{IRM}_{4.5\text{T}}$ (Table 1). After reaching $\text{IRM}_{4.5\text{T}}$, backfield was applied and H_{CR} was about 268 mT. High values of H_{CR} are expected for this kind of mineral, and, effectively, H_{CR} value determined for this sample is similar to characteristic values of hematite. The S-ratio was calculated (~ 0.147). S-ratio values close to 1 indicate predominance of ferrimagnetic materials among magnetic contributions. On the other hand, in this case, S-ratio is closer to 0, which is consistent with the magnetic characteristics of the studied sample (antiferromagnetic). Table 1 shows a very good agreement between different ratios $S_{+40\text{mT}}$ ($\text{IRM}_{+40\text{mT}}/\text{IRM}_{2.4\text{T}}$), $S_{+100\text{mT}}$ ($\text{IRM}_{+100\text{mT}}/\text{IRM}_{2.4\text{T}}$) and $\text{IRM}_{4.5\text{T}}/\chi$. According to the flow charts for discriminate different magnetic minerals (Figure 1.7 in Maher *et al.*, 1999), IRM acquisition measurements and the value of $\text{IRM}_{4.5\text{T}}/\chi$ lower than 200 kA m^{-1} allow confirm, in qualitative way, the presence of goethite.

Magnetic demagnetisation of the sample, after reaching ARM, was almost total ($\sim 15\%$ of ARM, Figure 4); whereas a residual magnetisation, close to NRM value, could not be erased. The median destructive field MDF_{ARM} was about 62.29 mT. High values of MDF_{ARM} were found by AF demagnetisation, as well as a weak demagnetisation corresponding to a high $\text{IRM}_{2.4\text{T}}$. However, it is worth

Table 1

Several magnetic parameters measured and estimated for the studied sample Goeth1 and for other natural Goethites

	χ [10^{-5} m ³ kg ⁻¹]	$\kappa_{FD}^{\%}$ [%]	T_N [°C]	ARM [10^{-6} A m ² kg ⁻¹]	κ_{ARM} [10^{-5} SI]	MDF _{ARM} [mT]	IRM _{4.5T} [mA m ² kg ⁻¹]	S _{+40mT} [dimensionless]	S _{+100mT} [dimensionless]	S-ratio [dimensionless]	H _{CR} [mT]	ARM/IRM _{2.4T} [dimensionless]	ARM/ χ [kA m ⁻¹]	IRM _{4.5T} / χ [kA m ⁻¹]
Goeth1 (a)	38.9	0	~85.7	19.38	27.1	62.29	22.2	~0.006	~0.07	0.147	268	~0.0009	0.05	57.07
Natural Goethite (b)	26-280	-	60-170	5	-	-	~8; 50	0.005	0.02	-	-	0.01; 0.0001	1.0; 0.007	70

(a) This study.

(b) From Banerjee, 1970; Thompson and Oldfield, 1986; Hunt *et al.*, 1995; Maher and Thompson, 1999; Dearing, 1999; France and Oldfield, 2000.

mentioning that ARM could not correspond to the saturation value, so MDF_{ARM} parameter could be underestimated. Figure 4 also shows that $IRM_{2.4T}$ demagnetisation was incomplete; $IRM_{2.4T}$ was only reduced to ~75%; for this reason MDF_{IRM} could not be calculated. These results are expectable in this kind of material. It is necessary to apply very high AF in order to erase the $IRM_{2.4T}$ (although it is not always possible) in this case an effective method is thermal demagnetisation (Dunlop and Özdemir, 1997).

The temperature dependence of κ is shown in Figure 5. The heating curve was carried out from room temperature to 150°C, a pronounced peak (Hopkinson peak-like increase) is observed at 85.7°C followed by an important decrease (~60%) up to 106.6°C. According to the discussion triggered by Petrovsky and Kapicka (2005) about the determination of the Curie (Néel) temperature from the temperature dependence of κ , a critical temperature was estimated from the evidence of a Hopkinson peak just below T_N , being ~85.7°C. The value of critical temperature T_N is lower than those proposed by some authors (~120°C), however, the lowest values can be related with intrinsic characteristics of goethite, such as crystallinity, excess water and grain size, the presence of small quantities of impurities or isomorphous substitution (Özdemir and Dunlop, 1996; De Boer and Dekkers, 1998; Dearing, 1999; Maher *et al.*, 2004; Barrero *et al.*, 2006). Although the decrease of κ at T_N is significant, it is not enough to make it zero. Probably, other magnetic materials with higher critical temperatures are present in the sample. Such possibility was confirmed through thermal demagnetisation measurements.

Stepwise thermal demagnetisation of IRM and susceptibility curves are shown in Figure 6. Three phases are observed from the thermal demagnetisation curve and from its derived distribution (see bar plot in Figure 6). A small low temperature phase is removed between room temperature and 200°C and it can be identified as goethite. The second small phase is removed between 230 and 400°C and the third one shows the largest decay of the remanent magnetisation. At about the Néel temperature of hematite ($T_N = 675^\circ\text{C}$), the remanent magnetisation is just entirely removed, showing the presence of hematite. Although intergrown hematite/goethite aggregates and newly formed hematite cannot be discriminated from this curve, it is possible to observe the neoformation of hematite through susceptibility curve.

The presence of goethite is also supported from the susceptibility curve (Figure 6). Susceptibility measurements were conducted between steps in order to monitor changes in magnetic mineralogy, in particular, pronounced changes are observed between 250 and 400°C. Such behaviour can be due to the dehydroxylation of goethite to hematite that takes place at 200-400°C (Özdemir and Dunlop, 1996; Ruan *et al.*, 2001; Przepiera and Przepiera, 2003).

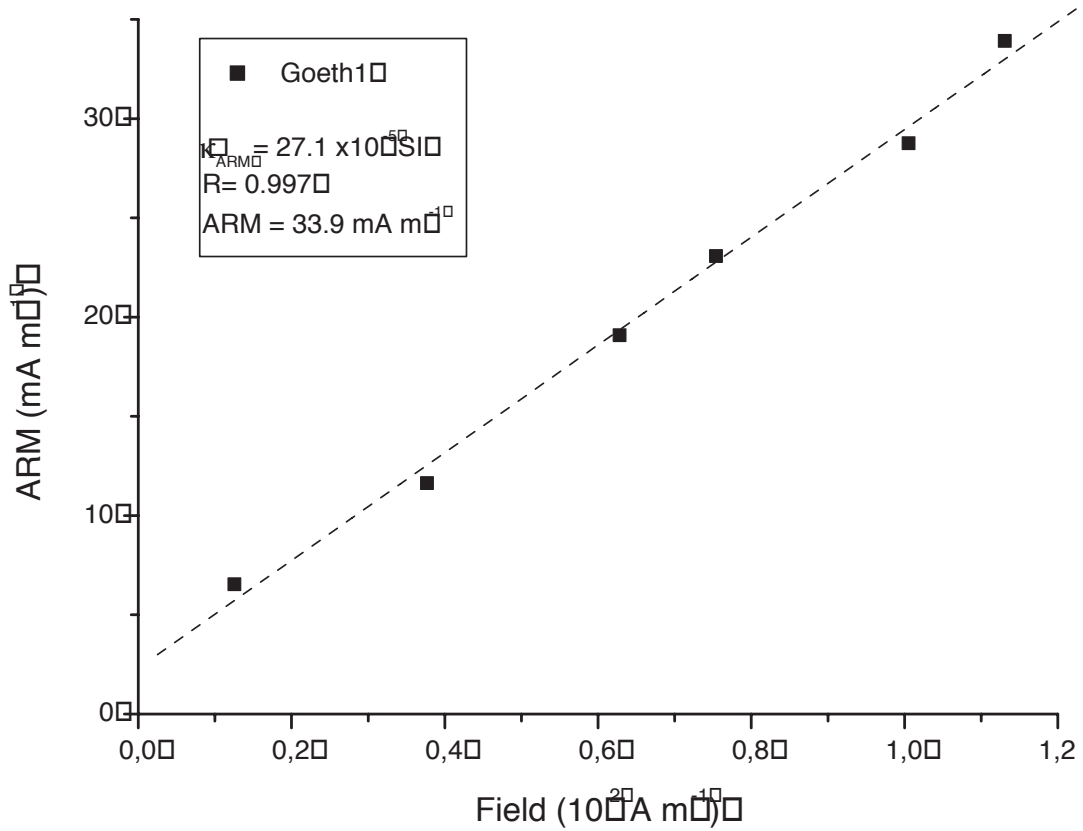


Fig. 2. ARM measurements. Values obtained for an AF= 100 mT, superimposing a DC field, that ranges between 10 and 90 μT , are shown. Saturation value of ARM was obtained from 90 μT DC field. κ_{ARM} was calculated from the curve slope.

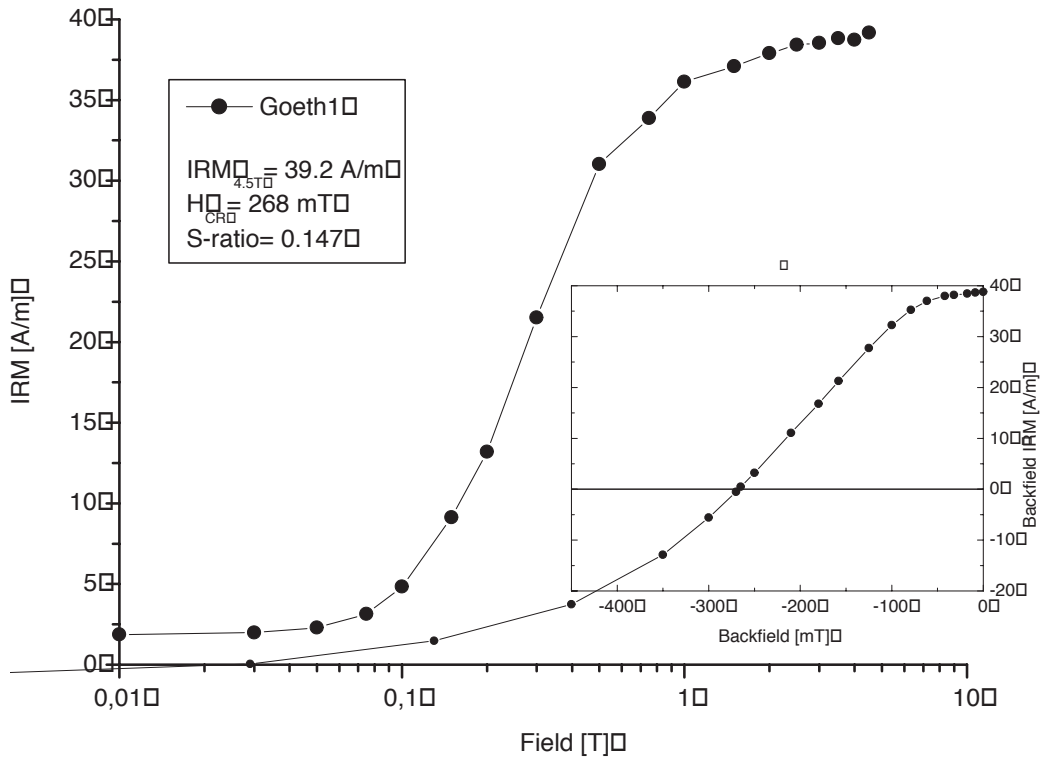


Fig. 3. IRM measurements. The highest applied field was 4.5 T. The following parameters were estimated: H_{CRD} , S-ratio, S_{+40mT} y S_{+100mT} .

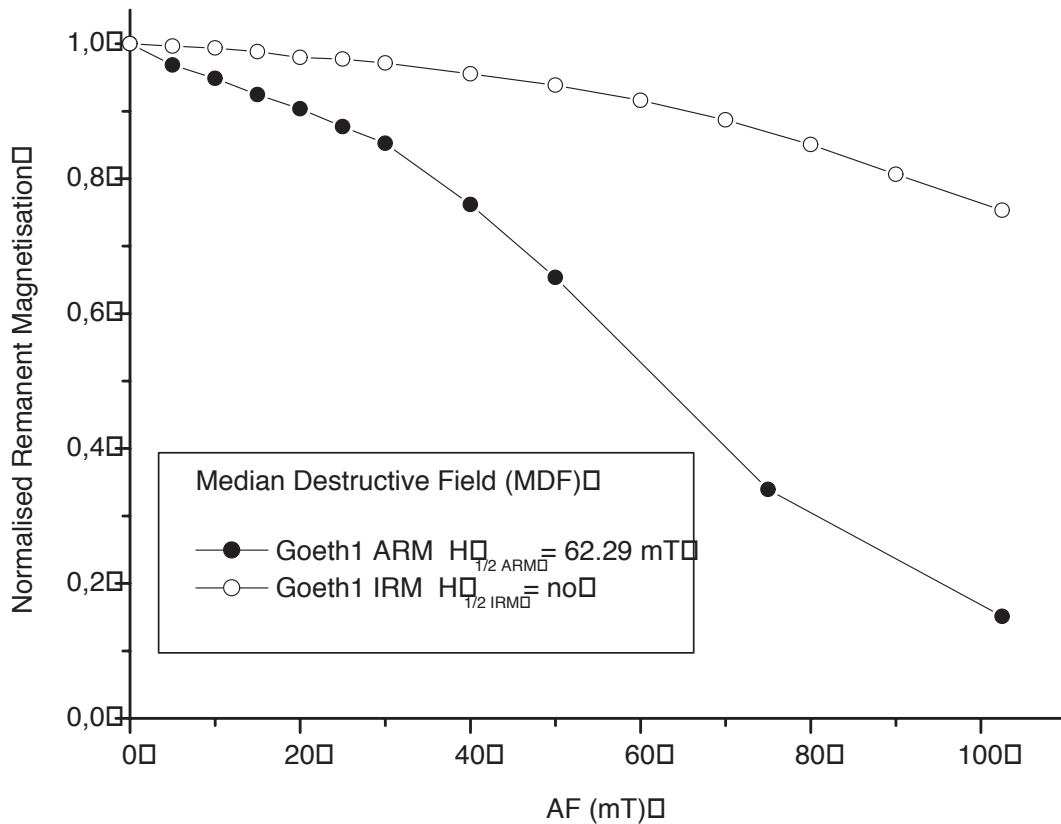


Fig. 4. AF demagnetisation. This process was applied on the sample after acquiring its ARM at 90 μT , and its IRM at 2.4 T.

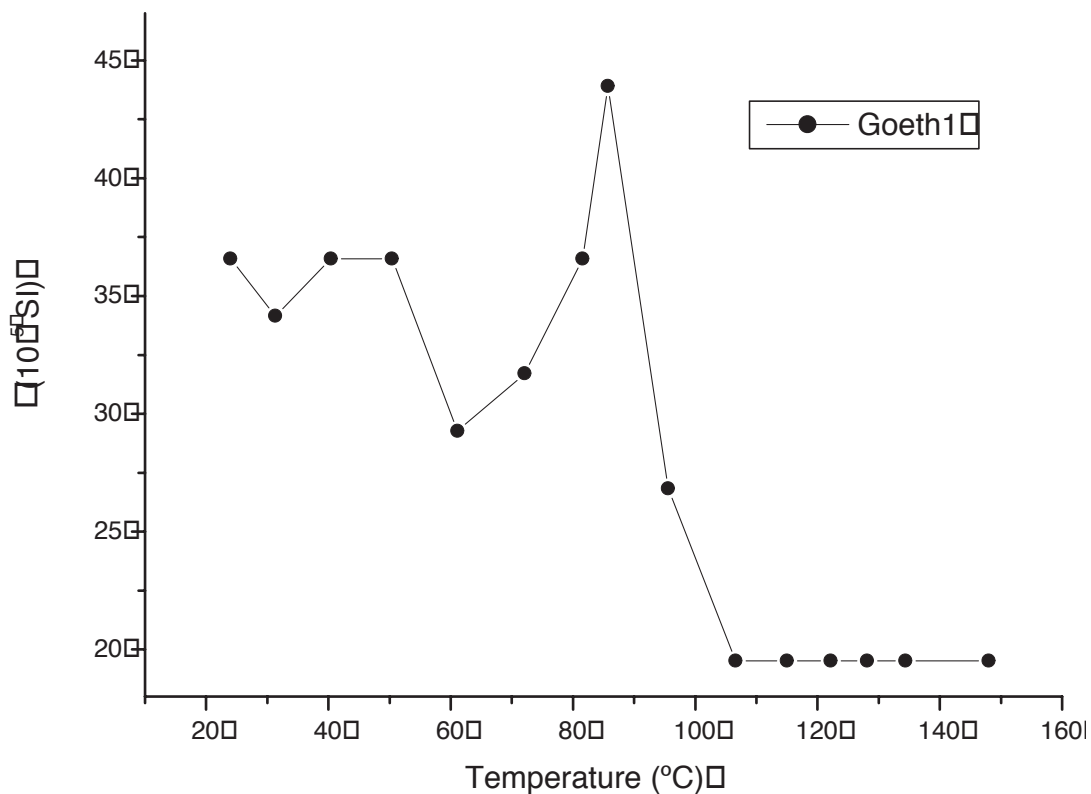


Fig. 5. Temperature dependence of susceptibility. A Hopkinson peak-like increase is observed at $\sim 85.7^\circ\text{C}$, followed by a pronounced decrease of the susceptibility.

Although in Tharsis area the main mineral is pyrite (FeS_2), its contribution to the magnetic parameters is not significant, on account of its paramagnetic nature. The presence of related iron sulphures, like pyrrhotite ($\sim\text{Fe}_7\text{S}_8$) and greigite (Fe_3S_4), common in this mine, is not observed in the studied sample, because the coercivity of remanence spectrum of these sulphures shows very much lower values than those calculated in this work (Sagnotti and Winkler, 1999). The magnetic susceptibility of pyrrhotite is also very much higher than those recorded in this study; moreover, this mineral and greigite were not detected from thermal studies. Although the presence of lepidocrocite is possible, the critical temperature of this mineral is -196°C , and at room temperature it has no remanent magnetisation (Thompson and Oldfield, 1986), then it does not contribute to the magnetic parameters. Finally, since magnetite is an iron oxide that occurs widely in most of environments, its presence should be discussed. This mineral is not inferred from room temperature magnetic measurements; moreover, any soft magnetic phase is not detected from stepwise thermal demagnetisation (Figure 6).

The material was also analysed by supportive studies, i.e. SEM and DRX techniques. Goethite of Tharsis mine

appears as pulverulent aggregates constituted by grains of irregular shape (Figure 7a), $10\text{-}20\ \mu\text{m}$ size, and sometimes as needle-like crystals, e.g. $\sim 3 \times 22\ \mu\text{m}$ (Figure 7b), in general with a poor crystalline development. The X ray diffraction diagram (Figure 8) shows that the analysed sample presents a high content of goethite with minor amounts of hematite and quartz revealed by the size and definition of the XRD peaks.

CONCLUSIONS

The presence of goethite in the material under study is confirmed from the analysis of different magnetic studies. Furthermore, its characteristic magnetic parameters were determined, contributing to new data of this mineral and its occurrence in Tharsis area. Since remanence studies of goethites, especially IRM, requires high fields to reach the saturation, related parameters (e.g.: coercivity of remanence) could be underestimated.

Although goethite is the mineral under interest, the presence of hematite – as intergrown goethite/hematite or neoformation after heating – cannot be discarded from IRM and thermal studies. On the other hand, traces of soft mineral,

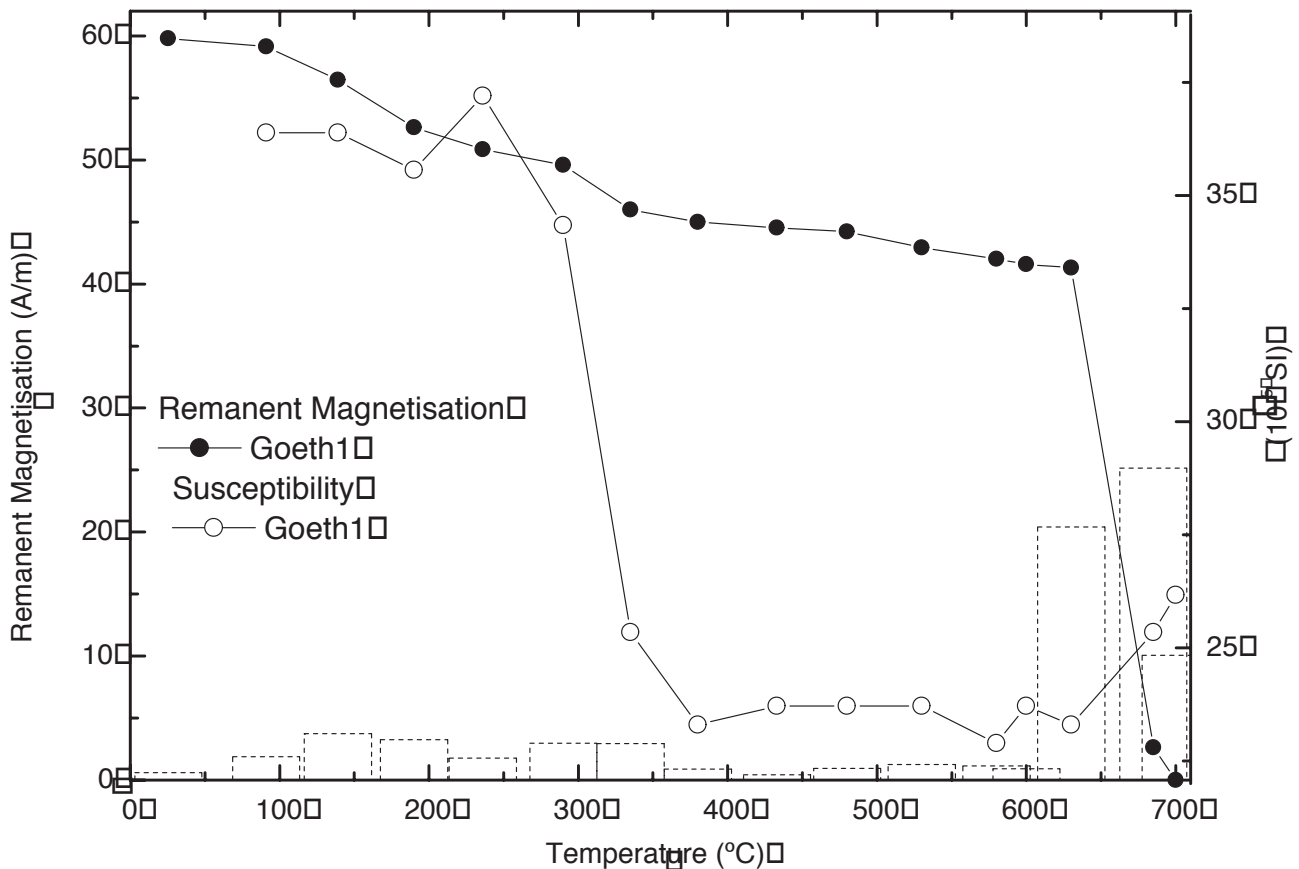


Fig. 6. Stepwise thermal demagnetisation of IRM and susceptibility curves. The bars plot represents the derived distribution (absolute values) of the remanent magnetisation.

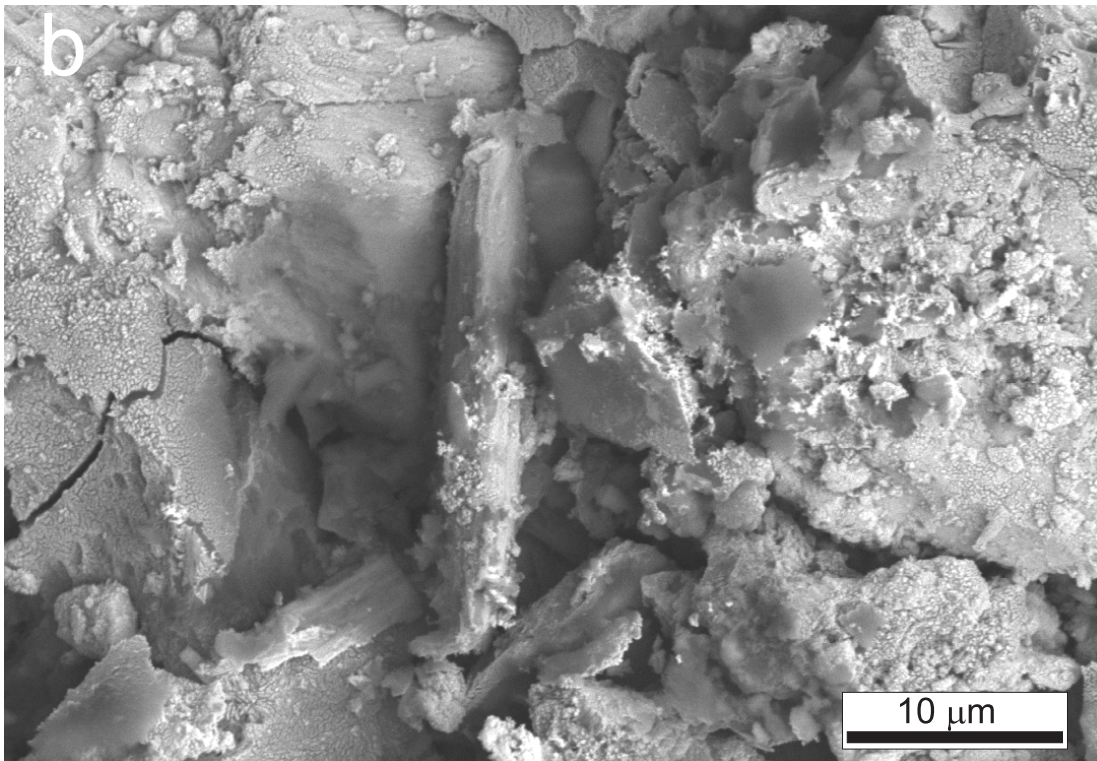
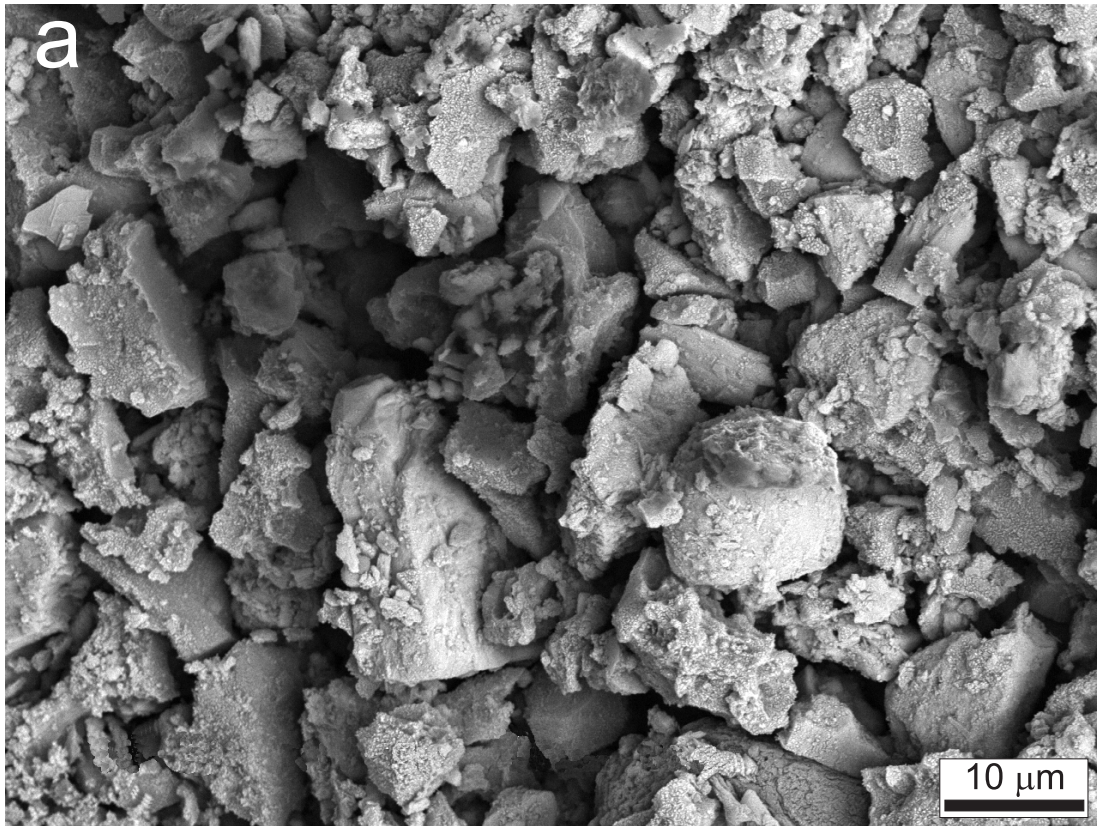


Fig. 7. Back scattered electron images (SEM) of goethite aggregates. a) pulverulent habit; b) needle-like crystal of goethite.

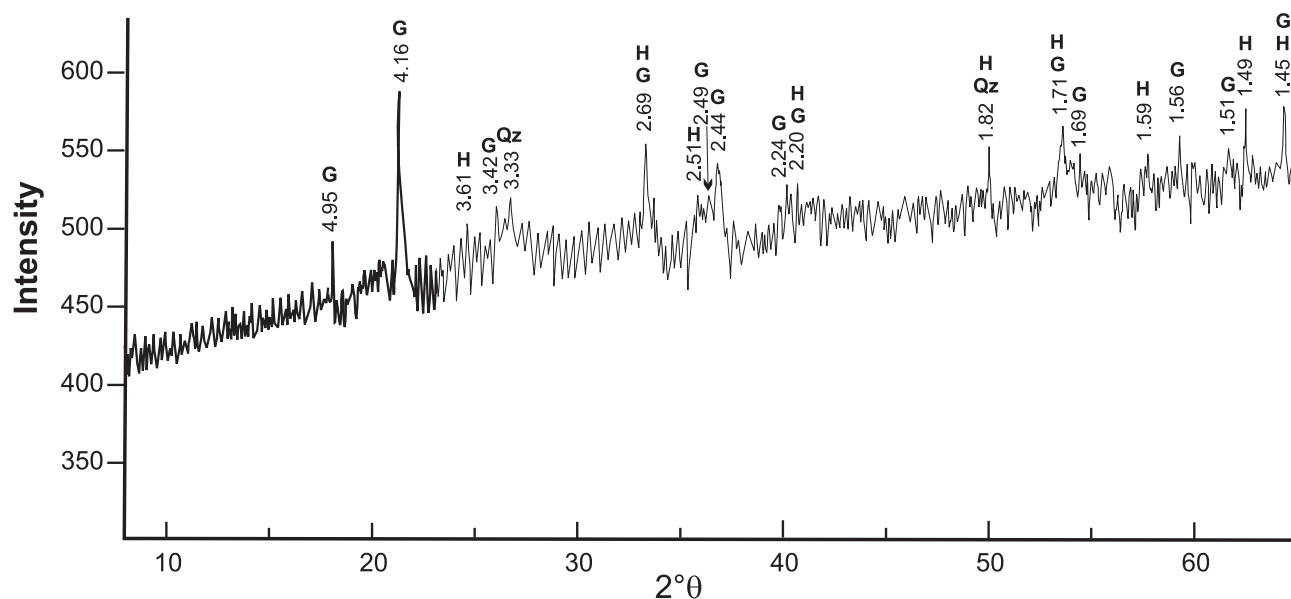


Fig. 8. Main peaks of X-ray diffraction analysis. G: goethite; H: hematite; Qz: quartz.

such as magnetite were not observed. In addition, such magnetic conclusions are supported by SEM and XRD studies.

ACKNOWLEDGEMENTS

The authors thank Universidad Nacional del Centro de la Provincia de Buenos Aires (UNCPBA), Universidad Nacional de La Plata (UNLP), CONICET and CICPBA for their financial support. Many thanks to Ing. Eduardo Tavani (Cetmic-CIC) for providing the material from Tharsis mine. The authors also thank to both anonymous reviewers for their useful suggestions in order to improve this manuscript.

BIBLIOGRAPHY

BANERJEE, S.K., 1970. Origin of thermoremanence in goethite. *Earth Planet Sci. Lett.* 8, 197-201.

BARRERO, C. A., J. D. BETANCUR, J. M. GRENECHE and T. S. BERQUÓ, 2006. Magnetism in non-stoichiometric goethite of varying total water content and surface area. *Geophys. J. Int.* 164 (2), 331-339.

DE BOER, C. B. and M. J. DEKKERS, 1998. Thermomagnetic behaviour of hematite and goethite as a function of grain size in various non-saturating magnetic fields. *Geophys. J. Int.* 133, 541-552.

DIXON, C., 1979. Atlas of Economic Mineral Deposits. Edited by Chapman and Hall Ltd., 68-69.

DEARING, J., R. DANN, K. HAY, J. LEES, P. LOVELAND, B. MAHER and K. O'GRADY, 1996.

Frequency-dependent susceptibility measurements of environmental materials. *Geophys. J. Int.* 124, 228-240.

DEARING, J., 1999. Operation manual, Bartington Instruments Ltd. Environmental magnetic susceptibility – Using the Bartington MS2 system. Chi Publishing, UK, 54 pp.

DEKKERS, M. J., 1989. Magnetic properties of natural goethite – I. Grain size dependence of some low- and high-field related rock magnetic parameters measured at room temperature. *Geophys. J.*, 97, 341-355.

DUNLOP, J. and Ö. ÖZDEMİR, 1997. Rock magnetism. Fundamentals and frontiers. Cambridge University Press. 573 pp.

EVANS, M. E. and F. HELLER, 1994. Magnetic enhancement and palaeoclimate: Study of a loess/palaeosol couplet across the Loess Plateau of China. *Geophys. J. Int.*, 117, 257-264.

FASSBINDER, J. W. E., H. STANJEK and H. VALI, 1990. Occurrence of magnetic bacteria in soil. *Nature*, 343, 161-163.

FINE, P., K. L. VEROSUB and M. J. SINGER, 1995. Pedogenic and lithogenic contributions to the magnetic susceptibility record of the Chinese loess/palaeosol sequence. *Geophys. J. Int.*, 122, 97-107.

FRANCE, D. E. and F. OLDFIELD, 2000. Identifying goethite and hematite from rock magnetic measurements of soils and sediments. *J. Geophys. Res.* 105, 2781-2795.

- HANESCH, M., H. STANJEK and N. PETERSEN, 2006. Thermomagnetic measurements of soil iron minerals: the role of organic carbon. *Geophys. J. Int.*, 165, 53-61.
- HEDLEY, I. G., 1971. The weak ferromagnetism of goethite (-FeOOH). *Z. Geophys.*, 37, 409-420.
- HUNT, C. P., B. M. MOSKOWITZ and S. K. BANERJEE, 1995. Magnetic properties of rocks and minerals. In: *Rock Physics and Phase Relations: A Handbook of Physical Constants*, 3, Ahrens, T. J., 189-204. American Geophysical Union, Washington, DC.
- JACKSON, M., W. GRUBER, J. MARVIN and S. K. BANERJEE, 1988. Partial anhysteretic remanence and its anisotropies: applications and grain-size-dependence. *Geophys. Res. Lett.*, 15, 440-443.
- KRUIVER, P. P., M. J. DEKKERS and D. HESLOP, 2001. Quantification of magnetic coercivity components by the analysis of acquisition curves of isothermal remanent magnetisation. *Earth Planet. Sci. Lett.*, 189, 269-276.
- LIU, X-M., J. SHAW, T-S. LIU, F. HELLER and M-Y. CHENG, 1993. Rock magnetic properties and palaeoclimate of Chinese loess. *J. Geomag. Geoelec.*, 45, 117-124.
- MAHER, B.A., 1986. Characterisation of soil by mineral magnetic measurements. *Phys. Earth Planet. Int.*, 42, 76-92.
- MAHER, B. A. and R. THOMPSON, 1999. Quaternary climates, environments and magnetism. Cambridge University Press. 390 pp.
- MAHER, B. A., V. V. KARLOUKOVSKI and T. J. MUTCH, 2004. High-field remanence properties of synthetic and natural submicrometre haematites and goethites: significance for environmental contexts. *Earth Planet. Sci. Lett.*, 226, 491- 505.
- MULLINS, C. E., 1973. Magnetic viscosity, quadrature susceptibility, and frequency dependence of susceptibility in single-domain assemblies of magnetite and maghemite. *J. Geophys. Res.*, 78 (5), 804-809.
- MULLINS, C. E., 1977. Magnetic susceptibility of the soil and its significance in Soil Science: a review. *J. Soil Sci.*, 28, 223-246.
- ÖZDEMİR, Ö. and D. J. DUNLOP, 1996. Thermoremanence and Néel temperature of goethite. *Geophys. Res. Lett.* 23, 921-924.
- PETROVSKY, E. and A. KAPICKA, 2005. Comments on "The use of field dependence of magnetic susceptibility for monitoring variations in titanomagnetite composition – a case study on basanites from the Vogelsberg 1996 drillhole, Germany" by de Wall and Nano, *Stud. Geophys. Geod.*, 48, 767-776. *Stud. Geophys. Geod.*, 49, 255-258.
- PRZEPIERA, K. and A. PRZEPIERA, 2003. Thermal transformations of selected transition metals oxyhydroxides. *J. Therm. Anal. Cal.*, 74, 659-666.
- ROCHETTE, P. and G. FILLION, 1989. Field and temperature behaviour of remanence in synthetic goethite: paleomagnetic implications. *Geophys. Res. Lett.*, 16 (8), 851-854.
- ROCHETTE P., L. ESTEBAN, H. RAKOTO, J-L., BOUCHEZ, Q. LIU and J. TORRENT, 2005. Non-saturation of the defect moment of goethite and fine-grained hematite up to 57 Tesla. *Geophys. Res. Lett.*, 32, L22309, doi:10.1029/2005GL024196.
- RUAN, H. D., R. L. FROST and J. T. KLOPROGGE, 2001. The behavior of hydroxyl units of synthetic goethite and its dehydroxylated product hematite. *Spectrochim. Acta, A*, 57, 2575-2586.
- SAGNOTTI, L. and A. WINKLER, 1999. Rock magnetism and paleomagnetism of greigite-bearing mudstones in the Italian peninsula. *Earth Planet. Sci. Lett.*, 165, 67-80.
- SOLOMON, M., F. TORNOS and O. C. GASPAR, 2002. Explanation for many of the unusual features of the massive sulphide deposits of the Iberian pyrite belt. *Geology*, 30 (1), 87-90.
- SANGODE, S. J., J. BLOEMENDAL, R. KUMAR and S. K. GHOSH, 2001. Plio-Pleistocene pedogenic changes in the Siwalik palaeosols: A rock magnetic approach. *Current Science*, 81 (4), 387-392.
- SANGODE, S. J. and J. BLOEMENDAL, 2004. Pedogenic transformation of magnetic minerals in Pliocene-Pleistocene palaeosols of the Siwalik Group, NW Himalaya, India. *Palaeogeography, Palaeoclimatology, Palaeoecology*, 212, 95-118.
- SCHWERTMANN, U., 1971. Transformation of hematite to goethite in soils. *Nature*, 232, 624-625.
- SCHWERTMANN, U., 1988. Occurrence and formation of iron oxides in various pedoenvironments. In: *Iron in*

- Soils and Clay Minerals, ed. Stucki, J.W. *et al.*, pp. 267-308. D. Reidel, Norwell, MA.
- STOCKHAUSEN, H., 1998. Some new aspects for the modelling of isothermal remanent magnetization acquisition curves by cumulative log Gaussian functions. *Geophys. Res. Lett.*, 25 (12), 2217-2220.
- STRAUSS, G. K. and J. MADEL, 1970. Geology of the Massive Sulphide Deposits in the Spanish – Portuguese pyrite Belt. *Geology*, 63,191-211.
- TARLING, D. and F. HROUDA, 1993. The magnetic anisotropy of rocks. Chapman and Hall. 217 pp.
- TAYLOR, R. M., B. A. MAHER and P. G. SELF, 1987. Magnetite in soils: I. The synthesis of single-domain and superparamagnetic magnetite. *Clay Minerals*, 22, 411-422.
- THOMPSON, R. and F. OLDFIELD, 1986. Environmental magnetism. Allen and Unwin (Publishers) Ltd. 225 pp.
- WALDEN, J., F. OLDFIELD and J. P. SMITH, (Eds) 1999. Environmental magnetism: a practical guide. Technical Guide, No. 6. Quaternary Research Association, London.
- WILLIAMS, E., 1933. The geology of the Río Tinto mines. *Transactions Institute Mining Metallurgy*, 43, 593-640.
- WILLIAMS, D., R. I. STATON and F. RAMBAAUD, 1975. The Planes-San Antonio pyretic deposit of Rio Tinto, Spain, its nature, environments and genesis. *Transactions Institute Mining Metallurgy*, 84, B73-B82.
-
- Marcos A.E. Chaparro^{1, *}, Ana M. Sinito¹, Juan C. Bidegain², Raúl E. de Barrio³
- ¹CONICET and IFAS, Universidad Nacional del Centro de la Provincia de Buenos Aires (UNCPBA), Pinto 399, 7000 Tandil (Argentina)
- ²CIC - LEMIT, calle 52 entre 121 y 122, 1900 La Plata (Argentina)
- ³Instituto de Recursos Minerales, Universidad Nacional de La Plata (UNLP), calle 64 N° 3 entre 119 y 120, 1900 La Plata (Argentina)

* Name and contact detail of the corresponding author:

Marcos A.E. Chaparro
IFAS, Universidad Nacional del Centro de la Provincia de Buenos Aires, Pinto 399, 7000 Tandil (Argentina)
Phone: +54 2293 439660. Fax: +54 2293 439669
Email: chaparro@exa.unicen.edu.ar